Molecular Vision 2015; 21:173-184 <http://www.molvis.org/molvis/v21/173>
Received 13 August 2014 | Accepted 17 February 2015 | Published 19 February 2015

Photoreceptor cells display a daily rhythm in the orphan receptor *Esrrβ*

Stefanie Kunst,[1,2] Tanja Wolloscheck,[1] Markus Grether,[1] Patricia Trunsch,[1] Uwe Wolfrum,[2] Rainer Spessert[1]

[1]Institute of Functional and Clinical Anatomy, University Medical Center of the Johannes Gutenberg University Mainz, Mainz, Germany; [2]Department of Cell and Matrix Biology, Institute of Zoology, Johannes Gutenberg University Mainz, Mainz, Germany

Purpose: Nuclear orphan receptors are critical for the development and long-term survival of photoreceptor cells. In the present study, the expression of the nuclear orphan receptor *Esrrβ*—a transcriptional regulator of energy metabolism that protects rod photoreceptors from dystrophy—was tested under daily regulation in the retina and photoreceptor cells.
Methods: The daily transcript and protein amount profiles were recorded in preparations of the whole retina and micro-dissected photoreceptor cells using quantitative PCR (qPCR) and western blot analysis.
Results: *Esrrβ* displayed a daily rhythm with elevated values at night in the whole retina and enriched photoreceptor cells. Daily regulation of *Esrrβ* mRNA depended on light input but not on melatonin, and evoked a corresponding rhythm in the Esrrβ protein.
Conclusions: The data presented in this study indicate that daily regulation of *Esrrβ* in photoreceptor cells may contribute to their adaptation to 24-h changes in metabolic demands.

In the mammalian retina, nuclear receptors complement other classes of transcriptional regulators in determining the fate of cells [1,2], their function [3,4], and homeostasis [5]. The majority of nuclear receptors found in the retina are so-called orphan receptors that are nuclear receptors with unknown physiologic ligands. Retinal nuclear orphan receptors typically control photoreceptor development and differentiation, and mutations result in dysfunction and degeneration of rod and/or cone photoreceptors [5]. A prominent example is the *retinoic acid-related orphan receptor beta* (*Rorβ*; OMIM 601972; Gene ID mouse 225998, Gene ID rat 309288) gene that directs the cell fate of rods and short (s)-opsin-expressing cones (S-cones) and controls the terminal differentiation of photoreceptor cells. Accordingly, mice mutant for *Rorβ* lack rods and gain primitive S-cones and photoreceptors lacking outer segments [6-8]. Among the nuclear orphan receptors, *estrogen-related receptor* β (*Esrrβ*, *Nr3b2*, OMIM 602167, Gene ID mouse 26380, Gene ID rat 299210) plays a special role. This orphan receptor does not detectably impair development but the long-term survival of photoreceptor cells instead. Thus, mice deficient for *Esrrβ* show slow and selective degeneration of rod photoreceptors in later life, which is preceded by the loss of rod outer segments [9]. Whereas mutations in nuclear orphan receptor genes often result in photoreceptor or ocular phenotypes, thus far only a few are known to underlie inherited retinal degeneration in humans [10-14]. Mutations in the human *Esrrβ* gene are associated with autosomal-recessive deafness [15] although investigations regarding vision disturbances have not yet been reported.

Mammalian photoreceptor cells must maintain their function for a lifetime in the face of hazards such as oxidative stress [16] and metabolic/energy challenges [17,18] occurring during the day/night cycle. To avoid age-related dysfunction or death, this may require the ability to adapt the cellular defense mechanisms and metabolism to 24-h changes in the environment [16]. Daily adaptation of photoreceptor cells (and other retinal neurons) is driven by light input and retinal clocks [19-21] through the release of the neuromodulators melatonin and dopamine, both of which play opposing roles in retinal adaptation [22]. Whereas melatonin is released during the dark/night and promotes dark-adaptive mechanisms [23-25], dopamine is released during the light/day and contributes to light adaptation of the photoreceptor cells [26,27].

At the transcriptional level, 24-h changes in the nuclear orphan receptor *Rorβ* contribute to daily adaptation of the retina and photoreceptor cells [28-30]. The data included in the present study show that daily changes of the nuclear orphan receptor *Esrrβ* are evident in photoreceptor cells and may contribute to their ability to comply with metabolic demands and thus to the cells' long-term survival.

Correspondence to: Rainer Spessert, Department of Functional and Clinical Anatomy, University Medical Center of the Johannes Gutenberg University Mainz, Saarstraße 19-21, 55099 Mainz, Germany, FAX: +49-6131-3923719; Phone: +49-6131-3923718; email: spessert@uni-mainz.de

METHODS

Animals: Animal experimentation was performed in accordance with the European Communities Council Directive (86/609/EEC). The study was approved by the German national investigation office and adhered to the ARVO Statement for Use of Animals in Research. Adult male and female rats (Sprague-Dawley) or mice (melatonin-proficient C3H/He, not carrying the *rd* mutation; melatonin-deficient C57BL/6Jb) were kept under standard laboratory conditions (illumination with fluorescent strip lights, 200 lux at cage level during the day and dim red light (<3 lux) during the night; 20±1 °C; water and food ad libitum) under 12 h:12 h light-dark (12:12 LD) for 3 weeks. When indicated, after LD treatment the animals were kept for one cycle under dim red light and killed during the next cycle. They were killed at the indicated time points by decapitation following anesthesia with 100% carbon dioxide for approximately 3 min. All dissections during the dark phase were performed under dim red light. The retinas were rapidly removed and immediately processed as follows.

Sample preparation: The sample size for all experiments was n=4, with each n deriving from 4 pooled retinas of 2 animals. The HEPES-glutamic acid buffer mediated organic solvent protection effect (HOPE; DCS, Hamburg, Germany) technique was applied to fix the retinas. Briefly, fixation started with the incubation of fresh retinas in an aqueous protection-solution HOPE I (DCS) for 48 h at 0–4 °C. Retinas were then dehydrated in a mixture of HOPE II solution (DCS) and acetone for 2 h at 0–4 °C, followed by dehydration in pure acetone for 2 h at 0–4 °C (repeated twice). Tissues were then embedded in low-melting paraffin (T_m=52–54 °C). Tissue sections (10 µm) from HOPE-fixed and paraffin-embedded retinas were prepared on membrane-mounted slides (DNase/RNase free PALM MembraneSlides, P.A.L.M., Bernried, Germany). Three sections were placed on each slide. The sections were deparaffinized with isopropanol (2 × 10 min each, at 60 °C). All sections were stained with cresyl violet (1% w/v cresyl violet acetate in 100% ethanol) for 1 min at room temperature, washed briefly in 70% and 100% ethanol, and then air-dried [31].

Laser microdissection and pressure catapulting: To isolate photoreceptor cells and inner retinal neurons from the stained sections in a contact- and contamination-free manner, the laser microdissection and pressure catapulting (LMPC) technique was applied [32]. The LMPC technique was performed using a PALM MicroBeam system (Zeiss MicroImaging, Munich, Germany) with PALM RoboSoftware (P.A.L.M.). Under the 10X objective, the outer nuclear layer bearing the photoreceptor cells and the tissue between the inner part of the outer plexiform layer and the inner ganglion cell layer bearing the inner retinal neurons were selected, cut, and catapulted into the caps of 0.5 ml microfuge tubes with an adhesive filling (PALM AdhesiveCaps, P.A.L.M.) by using a pulsed ultraviolet-A (UV-A) nitrogen laser. Smaller areas of the sections were pooled to reach total average sample sizes of 4 million square microns per tube. Alternatively, the whole retina was excised with a scalpel and collected in a 0.5 ml microfuge tube. Cell lysis for RNA preparation was performed immediately after the sample was collected. To verify the purity of the preparations, they were subjected to molecular analysis with rhodopsin (*Rho*) and neural retina leucine zipper (*Nrl*) as markers for photoreceptor cells and tyrosine hydroxylase (*Th*) and metabotropic glutamate receptor 6 (*mGluR6*) as markers for inner retinal neurons.

RNA extraction: RNA of the laser-microdissected tissue samples was isolated using the RNeasy Micro Kit (Qiagen, Hilden, Germany) following the manufacturer's instructions. Briefly, collected cells were lysed in a guanidine-thiocyanate-containing buffer (RLT buffer) supplied by the manufacturer. The lysates were diluted with RNase-free water and treated with proteinase K. The samples were then cleared with centrifugation, diluted with ethanol, and applied to a RNeasy MinElute Spin Column to bind RNA to the silica-gel membrane. After the first washing step, an on-column DNase treatment with RNase-free DNase I was performed as described by the manufacturer. Isolated RNA was eluted in the final volume of 12 µl RNase-free water. The amount of extracted RNA was determined by measuring the optical density at 260 and 280 nm.

Reverse-transcription and quantitative PCR: cDNA was synthesized using the Verso cDNA Kit (Abgene, Hamburg, Germany), following the manufacturer's instructions. Briefly, 4 µl RNA solution was reverse transcribed using anchored oligo-dT primers supplied with the kit in a final volume of 20 µl. cDNA was then diluted 1:3 in RNase-free water, and aliquots of 5 µl were used for PCR. Quantitative PCR was performed in a total volume of 25 µl containing 12.5 µl ABsolut QPCR SYBR Green Fluorescein Mix (Abgene), 0.75 µl of each primer (10 µM), 6 µl RNase-free water, and 5 µl sample. Primer sequences are listed in Table 1. PCR amplification and quantification were performed in a CFX96 (BioRad, Munich, Germany) according to the following protocol: denaturation for 3 min at 95 °C, followed by 40 cycles of 30 s at 95 °C, 20 s at 60 °C, and 20 s at 72 °C. All amplifications were performed in duplicate. By using agarose gel electrophoresis, the generated amplicons for all genes under examination were shown to possess the predicted sizes (Table 1). The amount of RNA was calculated from the measured threshold cycles (C_t) using a standard curve. The

transcript amount of glyceraldehyde-3-phosphate dehydrogenase (*Gapdh*) was constitutively expressed over the 24-h period in preparations of the whole retina, photoreceptor cells, and inner retinal neurons. Values were then normalized according to the amount of GAPDH mRNA present.

Western blot analysis: For western blot analysis, samples were loaded on 4–12% NuPAGE Novex Bis-Tris gels (Invitrogen, Carlsbad, CA), separated, and blotted onto polyvinylidene fluoride (PVDF) membrane (Westran S, Whatman Inc., Sanford, ME). For immunodetection, membranes were

Table 1. Primer sequences.

Gene	Accession number	Primer sequence 5′ to 3′	Product length of product [bp]PCR
r-Crx	NM_021855	F: GGCTGTCCCATACTCAAGTG	107
		R: GGTACTGGGTCTTGGCAAAC	
r-Esrrα	AY280663.1	F:GTGGCCGACAGAAGTACAAG	144
		R: CAACCACCAGCAGATGAGAC	
r-Esrrβ	NM_001008516	F: CAAGAGACGGCTGGATTCG	105
		R: TCGGCCACCAGTAGATACG	
m-Esrrβ	NM_011934	F: CCCTCGCCAACTCAGATTC	104
		R: GCGCTGACTCAGCTCATAG	
r-Esrrγ	AY341057	F: CTTGATCCTGGGTGTTGTG	101
		R: GGCCTGCTAATTTGGACTG	
r-Gapdh	NM_017008	F: ATGACTCTACCCACGGCAAG	89
		R: CTGGAAGATGGTGATGGGTT	
m-Gapdh	BC082592	F: GTCATCCCAGAGCTGAAC	144
		R: CTCAGATGCCTGCTTCAC	
r-mGluR6	NM_022920	F: ACAACCGCAGAAACATCTGG	113
		R: TTCCTCACCTGTGCATTTCC	
r-NeuroD	AF107728	F: AGACGAGTGCCTCAGTTC	136
		R: CTCCTCCAGATCCTCATCTTC	
r-Nr2c1	NM_145780	F: CGGAGAGGAGGAAGTTGTTG	126
		R: CGGGACTGAAGAGAACGATG	
r-Nr2e1	NM_001113197	F: GAGTTGACCGCTGTGTCTG	139
		R: CTGATTCGCACACGGACTC	
r-Nrl	NM_001106036	F: AGGCCTGGAGGAGCTATAC	134
		R: CATGAGGCCCTTCTACAGAG	
r-Nupr1	NM_053611	F: GCCTGGCCCAATCTTATGTC	116
		R: CTTGGTCAGCAGCTTCCTC	
r-Otx2	NM_001100566	F: CAGTCAATGGGCTGAGTC	112
		R: GCCCTCGTGAAAGTAGTC	
r-Rho	NM_033441	F: ACTCAGAAGGCAGAGAAGG	638
		R: CCTAGACACTTAGCCGTAAGC	
r-Rorβ	NM_001270958	F: GCCTGGCTGTTAGAACCAAG	147
		R: GTTGCAGACTGCCGTGATAG	
m-Rorβ	NM_001043354	F: CCTGGCTGATCGAACCAAG	144
		R: TGCAGACTGCCGTGATAG	
r-Th	NM_012740	F: CCAGGGCCTTTCCCAAAGTC	186
		R: CATGGAGGGCAGGAGGAATG	

blocked in 5% skimmed milk powder, and anti-Esrrβ polyclonal antibody (1:500; Abcam, Cambridge, MA; ab19331) was applied overnight at 4 °C. The horseradish-peroxidase-coupled secondary antibodies (goat anti-rabbit-HRP 1:5000; Sigma-Aldrich, St. Louis, MO; A0545) were visualized using an enhanced chemiluminescence (ECL) detection system (GE Healthcare Amersham, Freiburg, Germany). To ensure that immunoreactivity was derived from equal protein amounts of homogenates, staining with rabbit anti-β-actin polyclonal antibody (1:300; Sigma-Aldrich; A2066) was conducted. Densitometric measurement was performed using the ImageJ 1.46o software (National Institutes of Health, Bethesda, MD).

Statistical analysis: All PCR data are expressed as the mean ± standard error of the mean (SEM) of four independent experiments including eight time points. Transcript levels from each sample (consisting of four pooled retinas from two animals) were calculated relative to the average expression of each data set throughout 24 h to plot the temporal expression. Quantitative data were analyzed with ANOVA (one-way ANOVA) to evaluate variations among the groups. Cosinor analysis was used to fit sine-wave curves to the circadian data to mathematically estimate the time of peaking gene expression (acrophase) and to assess the amplitude [33,34]. The model can be expressed according to the following equation: $f(t)=A + B \cos [2\pi (t + C) / T]$. The f(t) indicates the relative expression levels of the target genes, t specifies the sampling time (h), A represents the mean value of the cosine curve (mesor; midline estimating statistic of rhythm), B indicates the amplitude of the curve (half of the sinusoid), and C indicates the acrophase (point of time, when the function f(t) is maximum). T gives the time of the period, which was fixed at 24 h for this experimental setting. The significance of the daily regulation was defined by showing $p<0.05$ in the ANOVA and Cosinor analysis.

RESULTS

Esrrβ mRNA and protein levels are under daily regulation in the retina: Nuclear orphan receptors important for the survival of photoreceptor cells or protective against photoreceptor dystrophy [5,35] were tested under daily regulation. Of the nuclear receptors considered under daily regulation (Figure 1, Table 2), only *Esrrβ* displayed a daily change in both statistical analyses applied (Figure 2, Table 3). The 24-h pattern of *Esrrβ* mRNA levels showed peak expression at ZT18.7 and an amplitude of 32.9%. Consistent with the validity of the results, the daily profile of the reference gene *Rorβ* was similar to those found in previous reports [28,30] (Figure 2, Table 3).

In the context of a putative role of *Esrrβ* in the protection of the retina against daily changes in the environment, the question of whether daily regulation of the *Esrrβ* gene results in daily changes in the protein product was addressed using western blotting (Figure 3). The anti-Esrrβ antibody recognizes a band of about 52 kDa, a molecular mass predicted from the *Esrrβ* gene. The intensity of Esrrβ immunoreactivity tended to increase during the light phase ($p=0.041$ in one-way ANOVA). This suggests that the daily rhythm in *Esrrβ* transcript levels evokes corresponding variations in the protein amount, with the temporal lag reflecting the time necessary to translate mRNA into protein.

Daily regulation of Esrrβ depends on illumination: Daily regulation of *Esrrβ* may be promoted by light input and/or a circadian clock. To investigate and compare the influence of both parameters between *Esrrβ* and *Rorβ*, rats adapted to the 12 h:12 h light-dark cycle were kept in constant darkness (DD) for one cycle and recorded during the subsequent cycle (Figure 2, Table 3). Under these conditions, the daily rhythm in the transcript levels was not detected for *Esrrβ*. As expected for a component of a circadian clock [23] and as reported previously [30], the amount of *Rorβ* mRNA persisted to the cycle under DD even though the cycling amplitude was clearly decreased (Figure 2, Table 3).

Daily regulation of Esrrβ evoked by photoreceptor cells: To compare daily regulation of *Esrrβ* and *Rorβ* between photoreceptor cells and inner retinal neurons, the LMPC technique was applied [32]. The purity grades of the preparations obtained were verified by using specific gene markers of photoreceptor cells, namely, *Rho* and *Nrl* (as markers for rods [36,37]) and of inner retinal neurons, namely, *Th* (as a marker for amacrine cells [38]) and *mGluR6* (as a marker of ON-bipolar cells [39]). Compared to whole retina preparations, in the photoreceptor cells collected with LMPC, the ratio of *Rho* to *Th* and *mGluR6* increased 34-fold and 85-fold, respectively, and that of *Nrl* to *Th* and *mGluR6* increased 170-fold and 43-fold, respectively. For the inner retina sample, the ratio of *Th* to *Rho* and *Nrl* increased 23-fold and 29-fold, respectively, and that of *mGluR6* to *Rho* and *Nrl* increased 15 fold and 18 fold, respectively.

To match the expression of the nuclear orphan receptors in the photoreceptor cells and the inner retinal neurons, mRNA levels were compared at the ZT of respective peak expression (Table 4). Both genes displayed higher transcripts in photoreceptor cells than in inner retinal neurons (*Esrrβ*: 23-fold; *Rorβ*: 15-fold). A comparison of the genes within the same tissue revealed that *Esrrβ* displayed higher transcript levels in photoreceptor cells (30-fold) and inner retinal neurons (15-fold).

To define and compare daily regulation of *Esrrβ* and *Rorβ* in photoreceptor cells and inner retinal neurons, the transcript levels were profiled in microdissected preparations of photoreceptor cells and inner retinal neurons. Both nuclear orphan receptors displayed daily rhythms in photoreceptor cells (Figure 4, Table 5) with similar 24-h profiles observed in preparations of the whole retina (Figure 2, Table 3). In contrast, the nuclear orphan receptors showed non-rhythmic expression in the inner retinal neurons (Figure 4, Table 5). These data suggest that the daily regulation of both genes in the retina is evoked primarily by photoreceptor cells.

Daily regulation of Esrrβ does not depend on melatonin: To investigate the contribution of melatonin to daily changes in the expression of *Esrrβ*, the 24-h course of the transcript levels of *Esrrβ* were compared between melatonin-proficient (C3H/He, not carrying the *rd* mutation) and melatonin-deficient mice (C57BL/6Jb; Figure 5, Table 6). The daily profiles of *Esrrβ* were similar in both mice strains and resembled that of rats (Figure 2, Table 3). As with *Esrrβ*, the reference gene *Rorβ* cycled in a similar manner in melatonin-proficient and -deficient mice. These observations suggest that daily regulation of *Esrrβ* and *Rorβ* does not require a pulsatile melatonin signal.

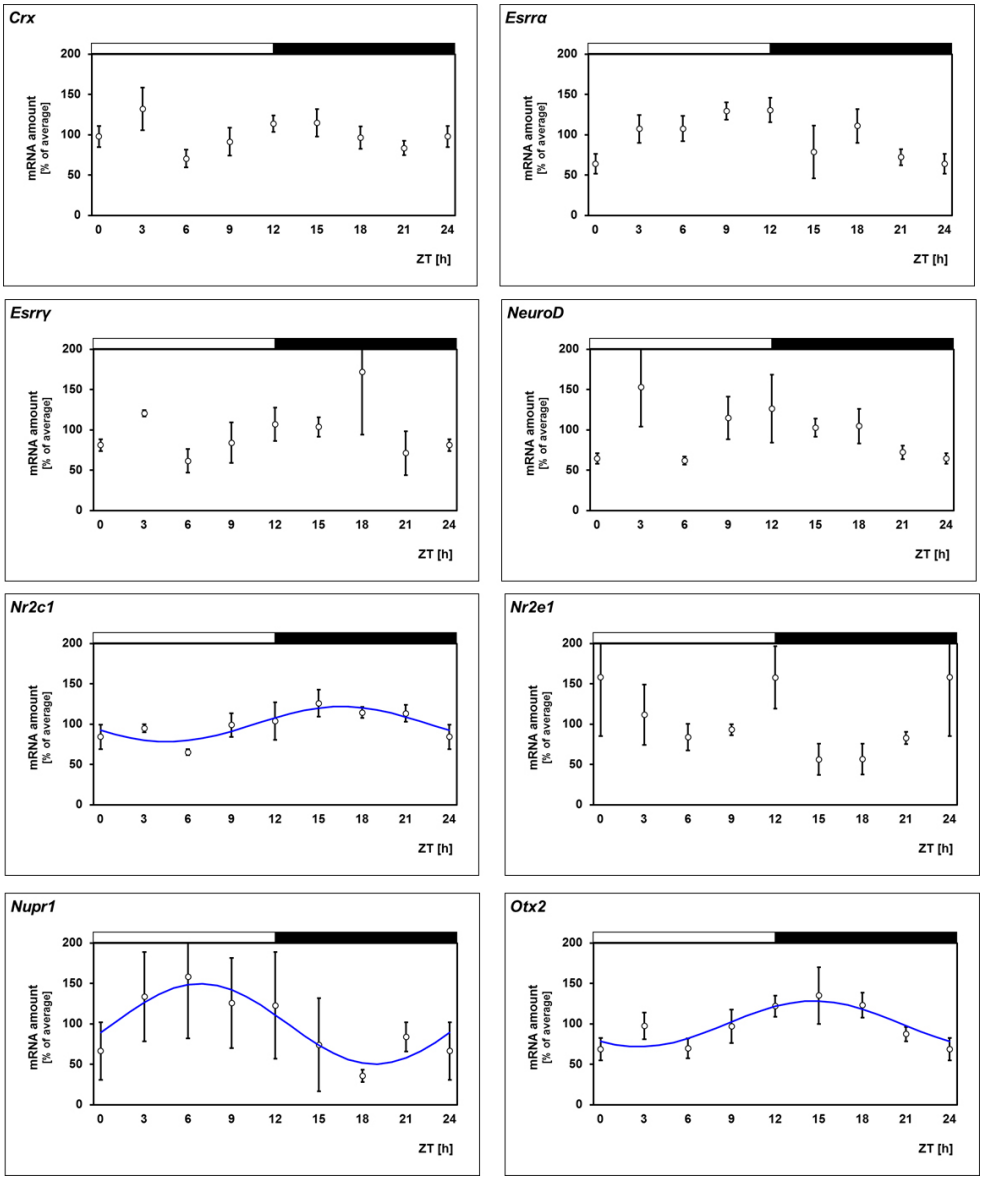

Figure 1. Twenty-four-hour profiling of various nuclear orphan receptors in preparations of the whole rat retina under 12 h:12 h light-dark cycles. The mRNA levels are plotted as a function of Zeitgeber time (ZT). The blue lines represent the periodic sinusoidal functions (illustrated only for $p<0.05$ in cosinor analysis). The solid bars indicate the dark period. Data represent a percentage of the average transcript amount during the 24-h period. The value of ZT0 was plotted twice at ZT0 and ZT24. Each value represents mean ± standard error of the mean (SEM; n=4). Statistical analysis of transcriptional profiling is provided in Table 2.

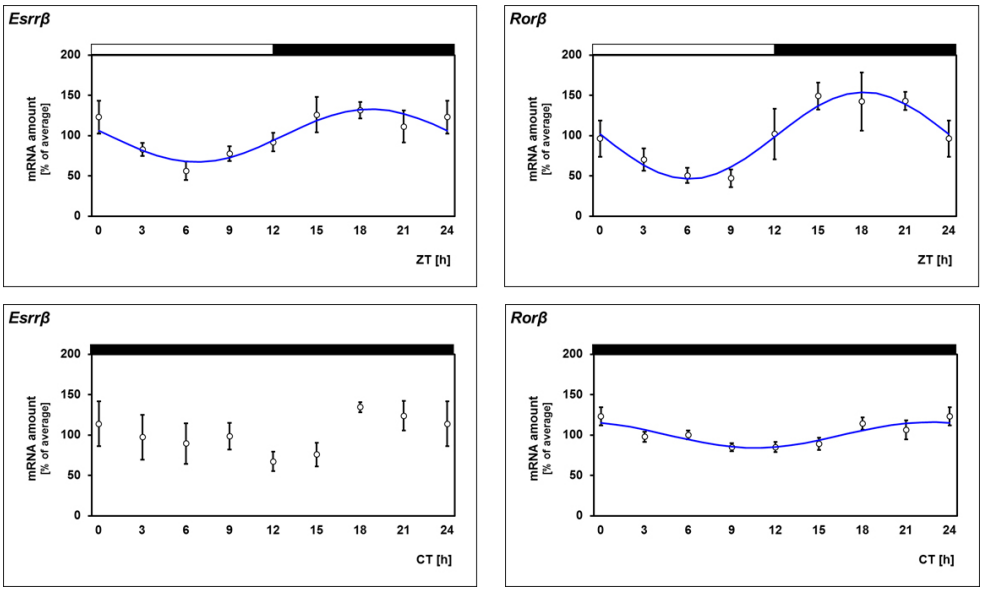

Figure 2. Twenty-four-hour profiling of *Esrrβ* and the reference gene *Rorβ* in preparations of whole rat retina under 12 h:12 h light-dark cycles (LD; upper line) or constant darkness (DD; lower line) using qPCR. The mRNA levels are plotted as a function of Zeitgeber time (ZT) and circadian time (CT). The blue lines represent the periodic sinusoidal functions determined with cosinor analysis (only for $p<0.05$). The solid bars indicate the dark period. Data represent a percentage of the average value of the transcript amount during the 24-h period. The value of ZT0 was plotted twice at ZT0 and ZT24. Each value represents mean ± standard error of the mean (SEM; n=4). Statistical analysis of transcriptional profiling is provided in Table 3. Note that daily rhythmicity of *Esrrβ* does not persist under DD.

Table 2. Statistical analysis of transcriptional profiling illustrated in Figure 1.

Gene	Whole retina under LD 12:12			
	One-way Anova	Cosinor analysis		
	P value	P value	Acrophase [h]	Amplitude [%]
Crx	=0.91	>0.05	-	-
Esrrα	=0.90	>0.05	-	-
Esrrγ	=0.86	>0.05	-	-
NeuroD	=0.90	>0.05	-	-
Nr2c1	=0.85	<0.05	16.6	21.8
Nr2e1	=0.95	>0.05	-	-
Nupr1	=0.72	<0.05	6.8	49.8
Otx2	=0.14	<0.05	14.7	28.3

Statistical analysis using one-way Anova and Cosinor analysis are shown for each gene under LD 12:12. (LD 12:12: light/dark 12:12)

Table 3. Statistical analysis of transcriptional profiling illustrated in Figure 2.

Gene	Whole retina under LD 12:12				Whole retina under DD			
	One-way Anova	Cosinor analysis			One-way Anova	Cosinor analysis		
	P value	P value	Acrophase [h]	Amplitude [%]	P value	P value	Acrophase [h]	Amplitude [%]
Esrrβ	=0.016	<0.05	18.7	32.9	=0.28	>0.05	-	-
Rorβ	=0.006	<0.05	18.1	53.9	=0.021	<0.05	22.6	15.9

Statistical analysis using one-way Anova and Cosinor analysis are shown for each gene under LD 12:12 and DD. (LD 12:12: light/dark 12:12; DD: constant darkness)

Table 4. Comparison of peak mRNA levels between photoreceptor cells (PRC) and the inner retina neurons.

Gene	PRC	Inner retina	PRC/inner retina ratio
Esrrβ	143,000	6.290	22.73
Rorβ	4530	296	15.30

Transcript amount was determined by qPCR and represents the number of transcripts in relation to *Gapdh* x 10^5 (mean ± SEM with n=4). (PRC: photoreceptor cells)

DISCUSSION

In this study, *Esrrβ* expression was observed under daily regulation in the retina. This indicates that cyclicity of *Esrrβ* is evident not only in peripheral tissues (such as white adipose tissue, brown adipose tissue, the liver, and muscle [40]) but also in the retina and thus in an area of the brain. The temporal timing of *Esrrβ* expression in the retina is similar to that found in both types of adipose tissues and is phase-advanced to that observed in the liver and muscle [40]. The retina resembles the peripheral tissues with *Esrrβ* cyclicity in its high metabolic activity and energy demand [41]. Therefore, daily regulation of *Esrrβ* may be a characteristic feature of tissues with high metabolic demand or may even be unique to them.

In the retina, the daily cyclicity of *Esrrβ* is evoked by photoreceptor cells. This is evident from the finding that the microdissected photoreceptor cells showed a daily rhythm in *Esrrβ*, which is similar to that observed in preparations of the whole retina, whereas microdissected inner retinal neurons did not appear to display *Esrrβ* rhythmicity at all. Although the high-purity grade of the photoreceptor preparations used was proven by the enrichment of transcripts known to be

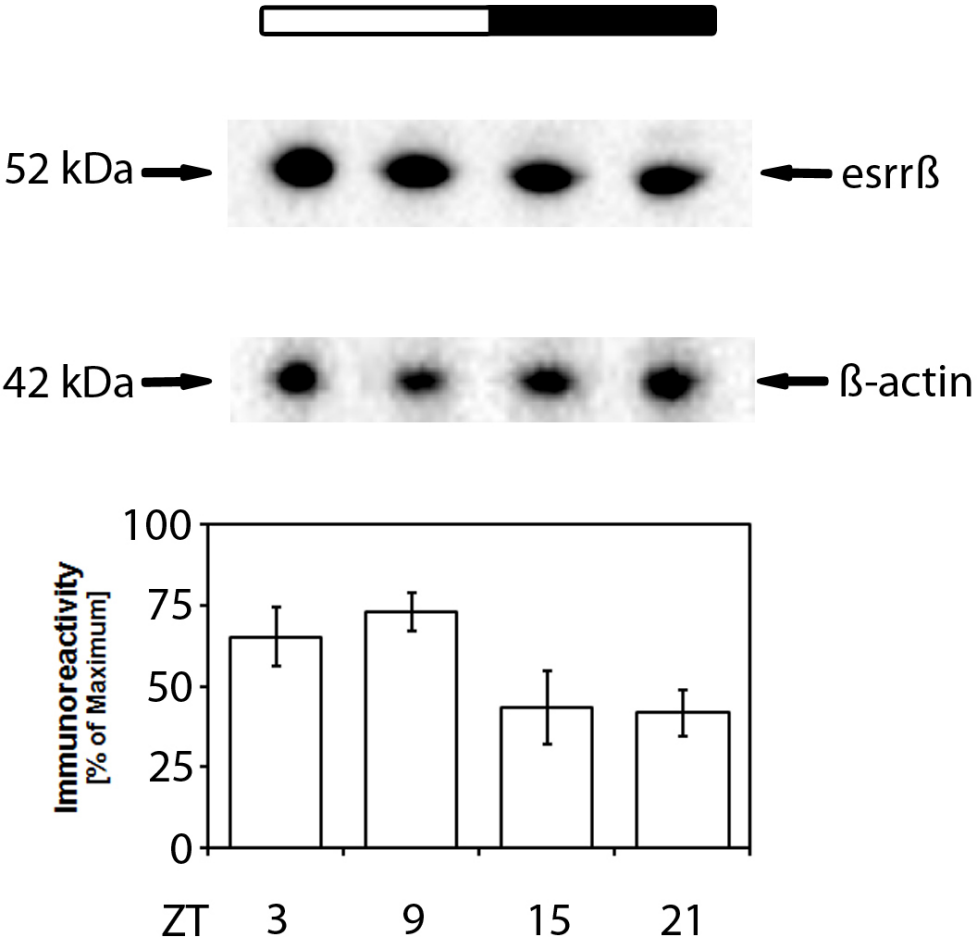

Figure 3. Western blot analysis of Esrrβ conducted at different ZTs (Zeitgeber times) during the 24-h cycle in the whole rat retina. The upper lanes show a representative western blot with Esrrβ immunostaining at about 52 kDa. The lower lanes show the β-actin signal to which the Esrrβ immunostaining was normalized. The diagram shows the quantification of immunoreactivity in relation to the corresponding β-actin signal. The solid bar indicates the dark period in the 12 h:12 h light-dark cycles. Data were obtained with densitometric measurement and represent percentages of the overall maximal value. Each value is the mean ± standard error of the mean (SEM; n=4). Note that Esrrβ immunoreactivity is elevated during the light phase (p=0.041 in one-way ANOVA).

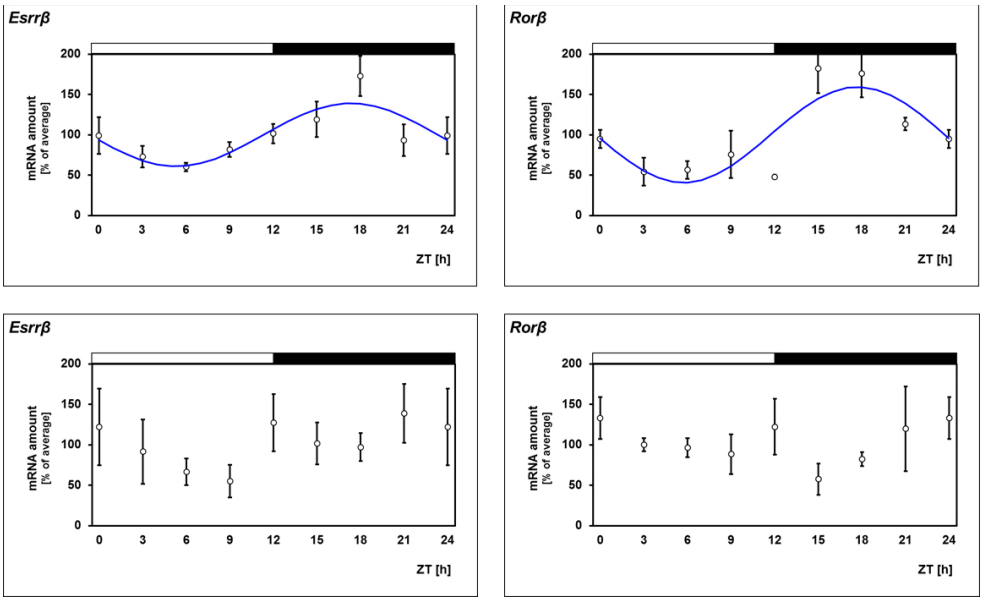

Figure 4. Comparative 24-h profiling of *Esrrβ* and the reference gene *Rorβ* in preparations of photoreceptor cells (upper line) and inner retinal neurons (lower line) of rats. The mRNA levels are determined by using quantitative PCR (qPCR), and both are plotted as a function of Zeitgeber time (ZT). The blue lines represent the periodic sinusoidal functions determined with cosinor analysis (only for $p<0.05$). The solid bars indicate the dark period. Data represent a percentage of the average transcript amount during the 24-h period. The value of ZT0 was plotted twice at ZT0 and ZT24. Each value represents mean ± standard error of the mean (SEM; n=4). Statistical analysis of transcriptional profiling is provided in Table 5. Note that daily variations of *Esrrβ* are evoked by photoreceptor cells.

specifically abundant in photoreceptor cells (*Rho*, *Nrl*), a limitation of this study is that the photoreceptor preparations were derived from rods and cones. Thus, the gene monitoring performed in the microdissected photoreceptors reflects the average rod and cone values and may not necessarily be valid for each photoreceptor type. However, *Esrrβ* was observed to be highly enriched in rod photoreceptors [42,43], and the *Esrrβ* mutation impairs only rod photoreceptors [9]. Therefore, daily regulation of *Esrrβ* probably occurs in rod photoreceptors.

Daily changes in *Esrrβ* require light-dark transitions and therefore depend on light input (this study) whereas that of *Rorβ* is truly circadian [30] (this study). This suggests that retinal nuclear orphan receptors on the whole mediate light-dependent and circadian adaptation. The rhythmicity of *Esrrβ* and *Rorβ* continued in melatonin-deficient mice and therefore does not require a pulsatile melatonin signal. As a result, neither the illumination-dependent regulation of *Esrrβ* nor the circadian regulation of *Rorβ* is mediated by melatonin.

Esrrβ influences the energy balance in the whole body [44] and is known to regulate key enzymes of fatty acid and carbohydrate metabolism in peripheral tissues [45] and photoreceptor cells [9]. Therefore, the cyclicity of *Esrrβ* may contribute to daily changes in the energy metabolism of the retina and photoreceptor cells and thus to their ability to adapt to 24-h changes in metabolic demands [17,18]. The fulfillment of metabolic demands appears to be a strong criterion in photoreceptor survival [46-48]. Thus, a role of *Esrrβ* in metabolic adaptation could (on a long-term basis) contribute to the survival of photoreceptor cells. This suggestion agrees with the observations that the loss of functional *Esrrβ* on a long-term basis leads to dysfunction and degeneration of rods and that enhanced *Esrrβ* activity rescues photoreceptor defects [9].

Table 5. Statistical analysis of transcriptional profiling illustrated in Figure 4.

Gene	PRCs under LD 12:12				IRN under LD 12:12			
	One-way Anova	Cosinor analysis			Oone-way Anova	Cosinor analysis		
	P value	P value	Acrophase [h]	Amplitude [%]	P value	P value	Acrophase [h]	Amplitude [%]
Esrrβ	=0.017	<0.05	17.3	39.0	=0.56	>0.05	-	-
Rorβ	=0.002	<0.05	17.7	59.3	=0.57	>0.05	-	-

Statistical analysis using one-way Anova and Cosinor analysis are shown for each gene in photoreceptor cells and inner retinal neurons. (LD 12:12: light/dark 12:12; PRC: photoreceptor cells; IRN: inner retinal neurons)

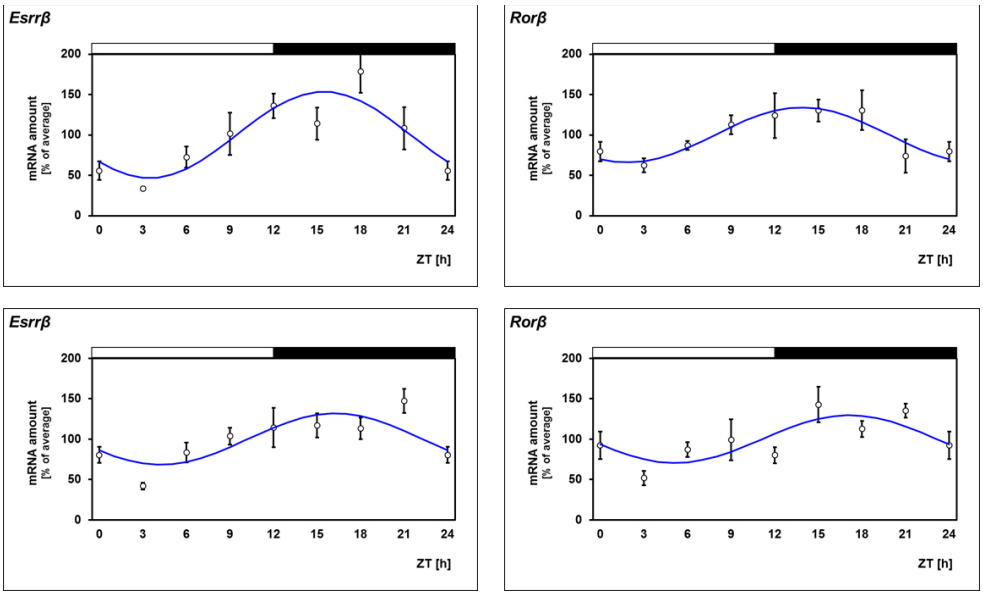

Figure 5. Comparative 24-h profiling of *Esrrβ* and *Rorβ* in the retina of melatonin-proficient (C3H/He, $rd^{+/+}$; upper line) and melatonin-deficient mice (C57BL/6J; lower line). The mRNA levels are determined by using quantitative PCR (qPCR), and both are plotted as a function of Zeitgeber time (ZT). The blue lines represent the periodic sinusoidal functions determined with cosinor analysis (only for $p<0.05$). The solid bars indicate the dark period. Data represent a percentage of the average value of the transcript amount during the 24-h period. The value of ZT0 was plotted twice at ZT0 and ZT24. Each value represents mean ± standard error of the mean (SEM; n=4). Statistical analysis of transcriptional profiling is provided in Table 6. Note that daily rhythmicity of *Esrrβ* does not depend on a pulsatile melatonin signal.

Similar to *Esrrβ*, the transcriptional coactivator *Pgc-1α* (i) protects photoreceptor cells from dystrophy [49], (ii) is under daily regulation in photoreceptor cells [50], and (iii) is important for metabolic homeostasis [51]. As a result, *Esrrβ* and *Pgc-1α* may act synergistically to increase photoreceptor survival through daily adjustment of its metabolism. Members of the *Esrr* family are coactivated by *Pgc-1α* to regulate energy metabolism in peripheral tissues [52]. If this occurs in photoreceptor cells, then *Esrrβ* and *Pgc-1α* may act jointly at the promoter level to maintain metabolic homeostasis of photoreceptor cells.

However, *Esrrβ* is known to target rod-specific genes including *Rho* [9]. Since *Rho* transcript levels are under daily regulation [28,53], this is consistent with the concept in which *Esrrβ* promotes the daily adaptation of rods by regulating rod-specific gene expression including that of *Rho*.

In conclusion, the data of the present study suggest a daily rhythm in *Esrrβ* expression that could promote metabolic adaptation of rods and in this way their long-term survival. Future investigations are required to investigate to what extent impairment of daily regulation of *Esrrβ* expression and energy metabolism may contribute to the various forms of photoreceptor dystrophy—in particular to those that are age-related.

ACKNOWLEDGMENTS

The authors thank Mr. Klaus Wolloscheck for statistical advice, Dr. Debra K. Kelleher for linguistic assistance, and Dr. Russell G. Foster for providing us with C3H/He (rd^{2+}) mice. We also thank Ms. Ute Frederiksen, Ms. Kristina Schäfer, Ms. Susanne Rometsch and Ms. Bettina Wiechers-Schmied for their excellent technical assistance and secretarial help. The data contained in this study are included in

Table 6. Statistical analysis of transcriptional profiling illustrated in Figure 5.

Gene	Melatonin proficient (C3H/He, $rd^{+/+}$)				Melatonin deficient (C57BL/6J)			
	One-way Anova	Cosinor analysis			One-way Anova	Cosinor analysis		
	P value	P value	Acrophase [h]	Amplitude [%]	P value	P value	Acrophase [h]	Amplitude [%]
Esrrβ	=0.016	<0.05	15.5	53.5	=0.001	<0.05	16.3	31.7
Rorβ	=0.041	<0.05	13.9	34.0	=0.006	<0.05	17.1	29.6

Statistical analysis using one-way Anova and Cosinor analysis are shown for each gene from samples of melatonin proficient and melatonin deficient mice.

the theses of Ms. Stefanie Kunst, Mr. Markus Grether and Ms. Patricia Trunsch as a partial fulfillment of their doctorate degree at the Johannes Gutenberg University, Mainz. The authors declare no conflicts of interest.

REFERENCES

1. Andreazzoli M. Molecular regulation of vertebrate retina cell fate. Birth Defects Res C Embryo Today 2009; 87:284-95. [PMID: 19750521].
2. Bassett EA, Wallace VA. Cell fate determination in the vertebrate retina. Trends Neurosci 2012; 35:565-73. [PMID: 22704732].
3. Yu RT, Chiang MY, Tanabe T, Kobayashi M, Yasuda K, Evans RM, Umesono K. The orphan nuclear receptor Tlx regulates Pax2 and is essential for vision. Proc Natl Acad Sci USA 2000; 97:2621-5. [PMID: 10706625].
4. Haider NB, Mollema N, Gaule M, Yuan Y, Sachs AJ, Nystuen AM, Naggert JK, Nishina PM. Nr2e3-directed transcriptional regulation of genes involved in photoreceptor development and cell-type specific phototransduction. Exp Eye Res 2009; 89:365-72. [PMID: 19379737].
5. Forrest D, Swaroop A. Minireview: the role of nuclear receptors in photoreceptor differentiation and disease. Mol Endocrinol 2012; 26:905-15. [PMID: 22556342].
6. André E, Conquet F, Steinmayr M, Stratton SC, Porciatti V, Becker-André M. Disruption of retinoid-related orphan receptor beta changes circadian behavior, causes retinal degeneration and leads to vacillans phenotype in mice. EMBO J 1998; 17:3867-77. [PMID: 9670004].
7. Srinivas M, Ng L, Liu H, Jia L, Forrest D. Activation of the blue opsin gene in cone photoreceptor development by retinoid-related orphan receptor beta. Mol Endocrinol 2006; 20:1728-41. [PMID: 16574740].
8. Jia L, Oh EC, Ng L, Srinivas M, Brooks M, Swaroop A, Forrest D. Retinoid-related orphan nuclear receptor RORbeta is an early-acting factor in rod photoreceptor development. Proc Natl Acad Sci USA 2009; 106:17534-9. [PMID: 19805139].
9. Onishi A, Peng GH, Poth EM, Lee DA, Chen J, Alexis U, de Melo J, Chen S, Blackshaw S. The orphan nuclear hormone receptor ERRbeta controls rod photoreceptor survival. Proc Natl Acad Sci USA 2010; 107:11579-84. [PMID: 20534447].
10. Haider NB, Jacobson SG, Cideciyan AV, Swiderski R, Streb LM, Searby C, Beck G, Hockey R, Hanna DB, Gorman S, Duhl D, Carmi R, Bennett J, Weleber RG, Fishman GA, Wright AF, Stone EM, Sheffield VC. Mutation of a nuclear receptor gene, NR2E3, causes enhanced S cone syndrome, a disorder of retinal cell fate. Nat Genet 2000; 24:127-31. [PMID: 10655056].
11. Sharon D, Sandberg MA, Caruso RC, Berson EL, Dryja TP. Shared mutations in NR2E3 in enhanced S-cone syndrome, Goldmann-Favre syndrome, and many cases of clumped pigmentary retinal degeneration. Arch Ophthalmol 2003; 121:1316-23. [PMID: 12963616].
12. Jacobson SG, Sumaroka A, Aleman TS, Cideciyan AV, Schwartz SB, Roman AJ, McInnes RR, Sheffield VC, Stone EM, Swaroop A, Wright AF. Nuclear receptor NR2E3 gene mutations distort human retinal laminar architecture and cause an unusual degeneration. Hum Mol Genet 2004; 13:1893-902. [PMID: 15229190].
13. Chavala SH, Sari A, Lewis H, Pauer GJ, Simpson E, Hagstrom SA, Traboulsi EI. An Arg311Gln NR2E3 mutation in a family with classic Goldmann-Favre syndrome. Br J Ophthalmol 2005; 89:1065-6. [PMID: 16024868].
14. Bernal S, Solans T, Gamundi MJ, Hernan I, de Jorge L, Carballo M, Navarro R, Tizzano E, Ayuso C, Baiget M. Analysis of the involvement of the NR2E3 gene in autosomal recessive retinal dystrophies. Clin Genet 2008; 73:360-6. [PMID: 18294254].
15. Collin RW, Kalay E, Tariq M, Peters T, van der Zwaag B, Venselaar H, Oostrik J, Lee K, Ahmed ZM, Caylan R, Li Y, Spierenburg HA, Eyupoglu E, Heister A, Riazuddin S, Bahat E, Ansar M, Arslan S, Wollnik B, Brunner HG, Cremers CW, Karaguzel A, Ahmad W, Cremers FP, Vriend G, Friedman TB, Riazuddin S, Leal SM, Kremer H. Mutations of ESRRB encoding estrogen-related receptor beta cause autosomal-recessive nonsyndromic hearing impairment DFNB35. Am J Hum Genet 2008; 82:125-38. [PMID: 18179891].
16. Du Y, Veenstra A, Palczewski K, Kern T. Photoreceptor cells are major contributors to diabetes-induced oxidative stress and local inflammation in the retina. Proc Natl Acad Sci USA 2013; 110:16586-91. [PMID: 24067647].
17. Ames A 3rd, Li YY. Energy requirements of glutamatergic pathways in rabbit retina. J Neurosci 1992; 12:4234-42. [PMID: 1359032].
18. Niven JE, Laughlin S. Energy limitations as a selective pressure on the evolution of sensory systems. J Exp Biol 2008; 211:1792-804. [PMID: 18490395].
19. Iuvone PM, Gan J, Alonso-Gomez AL. 5-Methoxytryptamine inhibits cyclic AMP accumulation in cultured retinal neurons through activation of a pertussis toxin-sensitive site distinct from the 2-[^{125}I] iodomalatonin binding site. J Neurochem 1995; 64:1892-5. [PMID: 7891120].
20. Ribelayga C, Mangel SC. Identification of a circadian clock-controlled neural pathway in the rabbit retina. PLoS ONE 2010; 5:e11020-[PMID: 20548772].
21. Green CB, Besharse JC. Retinal circadian clocks and control of retinal physiology. J Biol Rhythms 2004; 19:91-102. [PMID: 15038849].
22. McMahon DG, Iuvone PM, Tosini G. Circadian organization of the mammalian retina: From gene regulation to physiology and diseases. Prog Retin Eye Res 2014; 39:58-76. [PMID: 24333669].
23. Iuvone PM, Tosini G, Pozdeyev N, Haque R, Klein DC, Chaurasia SS. Circadian clocks, clock networks, arylalkylamine N-acetyltransferase, and melatonin in the retina. Prog Retin Eye Res 2005; 24:433-56. [PMID: 15845344].

24. Baba K, Pozdeyev N, Mazzoni F, Contreras-Alcantara S, Liu C, Kasamatsu M, Martinez-Merlos T, Strettoi E, Iuvone PM, Tosini G. Melatonin modulates visual function and cell viability in the mouse retina via the MT1 melatonin receptor. Proc Natl Acad Sci USA 2009; 106:15043-8. [PMID: 19706469].

25. Baba K, Mazzoni F, Owino S, Contreras-Alcantara S, Strettoi E, Tosini G. Age-related changes in the daily rhythm of photoreceptor functioning and circuitry in a melatonin-proficient mouse strain. PLoS ONE 2012; 7:e37799-[PMID: 22629458].

26. Iuvone PM, Galli CL, Garrison-Gund CK, Neff NH. Light stimulates tyrosine hydroxylase activity and dopamine synthesis in retinal amacrine neurons. Science 1978; 202:901-2. [PMID: 30997].

27. Witkovsky P. Dopamine and retinal function. Doc Ophthalmol 2004; 108:17-40. [PMID: 15104164].

28. Kamphuis W, Cailotto C, Dijk F, Bergen A, Buijs RM. Circadian expression of clock genes and clock-controlled genes in the rat retina. Biochem Biophys Res Commun 2005; 330:18-26. [PMID: 15781226].

29. Bai L, Zimmer S, Rickes O, Rohleder N, Holthues H, Engel L, Leube R, Spessert R. Daily oscillation of gene expression in the retina is phase-advanced with respect to the pineal gland. Brain Res 2008; 1203:89-96. [PMID: 18321474].

30. Sandu C, Hicks D, Felder-Schmittbuhl MP. Rat photoreceptor circadian oscillator strongly relies on lighting conditions. Eur J Neurosci 2011; 34:507-16. [PMID: 21771113].

31. Goldmann T, Burgemeister R, Sauer U, Loeschke S, Lang DS, Branscheid D, Zabel P, Vollmer E. Enhanced molecular analyses by combination of the HOPE-technique and laser microdissection. Diagn Pathol 2006; 1:2-[PMID: 16759346].

32. Schneider K, Tippmann S, Spiwoks-Becker I, Holthues H, Wolloscheck T, Spatkowski G, Engel L, Frederiksen U, Spessert R. Unique clockwork in photoreceptor of rat. J Neurochem 2010; 115:585-94. [PMID: 20722965].

33. Cornelissen G. Cosinor based rhythmometry. Theor Biol Med Model 2014; 11:16-[PMID: 24725531].

34. Refinetti R, Lissen GC, Halberg F. Procedures for numerical analysis of circadian rhythms. Biol Rhythm Res 2007; 38:275-325. [PMID: 23710111].

35. Mollema N, Haider NB. Focus on molecules: nuclear hormone receptor Nr2e3: impact on retinal development and disease. Exp Eye Res 2010; 91:116-7. [PMID: 20450910].

36. Mears AJ, Kondo M, Swain PK, Takada Y, Bush RA, Saunders TL, Sieving PA, Swaroop A. Nrl is required for rod photoreceptor development. Nat Genet 2001; 29:447-52. [PMID: 11694879].

37. Foster RG, Hankins MW, Peirson SN. Light, photoreceptors, and circadian clocks. Methods Mol Biol 2007; 362:3-28. [PMID: 17416998].

38. Osborne NN, Patel S, Vigny A. Dopaminergic neurones in various retinas and the postnatal development of tyrosine-hydroxylase immunoreactivity in the rabbit retina. Histochemistry 1984; 80:389-93. [PMID: 6145688].

39. Vardi N, Duvoisin R, Wu G, Sterling P. Localization of mGluR6 to dendrites of ON bipolar cells in primate retina. J Comp Neurol 2000; 423:402-12. [PMID: 10870081].

40. Yang X, Downes M, Yu RT, Bookout AL, He W, Straume M, Mangelsdorf DJ, Evans RM. Nuclear receptor expression links the circadian clock to metabolism. Cell 2006; 126:801-10. [PMID: 16923398].

41. Yu DY, Cringle SJ. Oxygen distribution and consumption within the retina in vascularised and avascular retinas and in animal models of retinal disease. Prog Retin Eye Res 2001; 20:175-208. [PMID: 11173251].

42. Blackshaw S, Fraioli RE, Furukawa T, Cepko CL. Comprehensive analysis of photoreceptor gene expression and the identification of candidate retinal disease genes. Cel. 2001; 107:579-89. [PMID: 11733058].

43. Blackshaw S, Harpavat S, Trimarchi J, Cai L, Huang H, Kuo WP, Weber G, Lee K, Fraioli RE, Cho SH, Yung R, Asch E, Ohno-Machado L, Wong WH, Cepko CL. Genomic analysis of mouse retinal development. PLoS Biol 2004; 2:E247-[PMID: 15226823].

44. Byerly MS, Al Salayta M, Swanson RD, Kwon K, Peterson JM, Wei Z, Aja S, Moran TH, Blackshaw S, Wong GW. Estrogen-related receptor β deletion modulates whole-body energy balance via estrogen-related receptor γ and attenuates neuropeptide Y gene expression. Eur J Neurosci 2013; 37:1033-47. [PMID: 23360481].

45. Giguère V. Transcriptional control of energy homeostasis by the estrogen-related receptors. Endocrine Re. 2008; 29:677-96. [PMID: 18664618].

46. Umino Y, Everhart D, Solessio E, Cusato K, Pan JC, Nguyen TH, Brown ET, Hafler R, Frio BA, Knox BE, Engbretson GA, Haeri M, Cui L, Glenn AS, Charron MJ, Barlow RB. Hypoglycemia leads to age-related loss of vision. Proc Natl Acad Sci USA 2006; 103:19541-5. [PMID: 17159157].

47. Punzo C, Kornacker K, Cepko CL. Stimulation of the insulin/mTOR pathway delays cone death in a mouse model of retinitis pigmentosa. Nat Neurosci 2009; 12:44-52. [PMID: 19060896].

48. Chertov AO, Holzhausen L, Kuok IT, Couron D, Parker E, Linton JD, Sadilek M, Sweet IR, Hurley JB. Roles of glucose in photoreceptor survival. J Biol Chem 2011; 286:34700-11. [PMID: 21840997].

49. Egger A, Samardzija M, Sothilingam V, Tanimoto N, Lange C, Salatino S, Fang L, Garcia-Garrido M, Beck S, Okoniewski MJ, Neutzner A, Seeliger MW, Grimm C, Handschin C. PGC-1α determines light damage susceptibility of the murine retina. PLoS ONE 2012; 7:e31272-[PMID: 22348062].

50. Kunst S, Wolloscheck T, Hölter P, Wengert A, Grether M, Sticht C, Weyer V, Wolfrum U, Spessert R. Transcriptional analysis of rat photoreceptor cells reveals daily regulation of genes important for visual signaling and light damage

susceptibility. J Neurochem 2013; 124:757-69. [PMID: 23145934].

51. Liu C, Lin JD. PGC-1 coactivators in the control of energy metabolism. Acta Biochim Biophys Sin (Shanghai) 2011; 43:248-57. [PMID: 21325336].

52. Scarpulla RC. Metabolic control of mitochondrial biogenesis through the PGC-1 family regulatory network. Biochim Biophys Acta 2011; 1813:1269-78. [PMID: 20933024].

53. von Schantz M, Lucas RJ, Foster RG. Circadian oscillation of photopigment transcript levels in the mouse retina. Brain Res Mol Brain Res 1999; 72:108-14. [PMID: 10521605].

Articles are provided courtesy of Emory University and the Zhongshan Ophthalmic Center, Sun Yat-sen University, P.R. China. The print version of this article was created on 19 February 2015. This reflects all typographical corrections and errata to the article through that date. Details of any changes may be found in the online version of the article.